Chemistry–A European Journal
Research Article
doi.org/10.1002/chem.202401233
Chemistry Europe
European Chemical Societies Publishing
www.chemeurj.org

Elucidating the Mechanism of Efficient Eu(III) and Yb(III) Sensitisation from a Re(I) Tetrazolato Triangular Assembly

Phillip J. Wright,[a] Michael C. Pfrunder,[b] Isaac M. Etchells,[b] Mohammad A. Haghighatbin,[c] Paolo Raiteri,[a] Mark I. Ogden,[a] Stefano Stagni,[d] Conor F. Hogan,[c] Lee J. Cameron,[a] Evan G. Moore,*[b] and Massimiliano Massi*[a]

The reaction of $Re(CO)_5Br$ with deprotonated 1*H*-(5-(2,2′:6′,2″-terpyridine)pyrid-2-yl)tetrazole yields a triangular assembly formed by tricarbonyl Re(I) vertices. Photophysical measurements reveal blue-green emission with a maximum at 520 nm, 32% quantum yield, and 2430 ns long-lived excited state decay lifetime in deaerated dichloromethane solution. Coordination of lanthanoid ions to the terpyridine units red-shifts the emission to 570 nm and also reveals efficient (90%) and fast sensitisation of both Eu(III) and Yb(III) at room temperature, with a similar rate constant k_{ET} on the order of 10^7 s^{-1}. Efficient sensitisation of Eu(III) from Re(I) is unprecedented, especially when considering the close proximity in energy between the donor and acceptor excited states. On the other hand, comparative measurements at 77 K reveal that energy transfer to Yb(III) is two orders of magnitude slower than that to Eu(III). A two-step mechanism of sensitisation is therefore proposed, whereby the rate-determining step is a thermally activated energy transfer step between the Re(I) centre and the terpyridine functionality, followed by rapid energy transfer to the respective Ln(III) excited states. At 77 K, the direct Re(I) to Eu(III) energy transfer seems to proceed via a ligand-mediated superexchange Dexter-type mechanism.

Introduction

The luminescent properties of trivalent lanthanoid (Ln) ions have been the focus of extensive investigation, both at fundamental and applied levels. In part, this interest originates from the many potential applications that luminescent lanthanoids find in various technologies such as optical displays, sensing, life sciences, and telecommunication signalling, to name a few.[1–5] The luminescent properties of these elements are quite distinct from those of transition metal complexes, due to the intrinsic properties associated with their valence 4*f* electrons. Ln(III) ions have typical line-like emission that is mostly dependent on the specific elements, ranging from the UV (e.g. Gd) and visible (e.g. Eu, Tb, Ho, Sm) to the NIR region (e.g. Yb, Nd, Er). This feature originates from the poor shielding and inner core nature of the 4*f* electrons.[6] Efficient luminescence of Ln(III) ions relies on their sensitisation via the antenna effect, due to the low molar absorptivity associated with Laporte-forbidden – and often spin-forbidden – intraconfigurational *f-f* electronic transitions.[7] In general, a chromophoric ligand absorbs incident energy and then transfers it to the Ln(III) cation. Most commonly, the chromophore is a π-conjugated organic system, bound or in proximity to the Ln centre, that is promoted to its singlet excited state, undergoes intersystem crossing to its triplet excited state, facilitated by the strong Ln-induced spin-orbit coupling, which then transfers the energy to the Ln(III) ion.[8] Although it is known that energy transfer (ET) can also occur via the singlet excited state,[9] sensitisation of Ln(III) ions is more often only considered as originating from the triplet excited state. Studies reported by Latva and co-workers have shown that efficient sensitisation relies on an optimal range of energy difference between the donor and acceptor states, which should be around 3500–2500 cm^{-1}.[10] Values below this range decrease the sensitisation efficiency as a result of thermally activated back energy transfer (BET).

Sensitisation of Ln(III) luminescence can occur from donors other than organic chromophores, such as lanthanoid-to-lanthanoid ET, for example Tb(III)→Eu(III), Eu(III)→Nd(III), or Yb(III)→Er(III).[11–13] Alternatively, sensitisation can originate from the charge transfer excited states of transition metal complexes (e.g. metal-to-ligand charge transfer, MLCT).[14–18] These sensitisation pathways have received comparatively less investigation. ET between transition metal complexes and lanthanoid ele-

[a] Dr. P. J. Wright, Prof. P. Raiteri, M. I. Ogden, L. J. Cameron, Prof. M. Massi
School of Molecular and Life Sciences
Curtin University
Perth, WA 6102, Australia
E-mail: m.massi@curtin.edu.au
[b] Dr. M. C. Pfrunder, I. M. Etchells, A/Prof. E. G. Moore
School of Chemistry and Molecular Biosciences
University of Queensland
Brisbane, QLD 4072, Australia
E-mail: egmoore@uq.edu.au
[c] Dr. M. A. Haghighatbin, Prof. C. F. Hogan
Department of Chemistry and Physics
La Trobe University
Melbourne, VIC 3086, Australia
[d] A/Prof. S. Stagni
Department of Industrial Chemistry "Toso Montanari"
University of Bologna
Bologna, 40136, Italy

Supporting information for this article is available on the WWW under https://doi.org/10.1002/chem.202401233

ments have predominantly focused on archetypal phosphorescent metal complexes containing Re(I),[19–22] Ru(II),[23–24] Os-(II),[25–26] Ir(III),[27–31] or Pt(II),[32–34] whereby sensitisation occurs from a triplet charge transfer excited state, ^{3}MLCT. Depending on the energy of the donor excited state, efficient sensitisation of both visible emitters, such as Eu(III), or NIR emitters, such as Yb(III), Nd(III), or Er(III), have been reported. However, detailed investigations on the mechanism of ET, which may occur via a Coulombic interaction (Förster) or electron exchange (Dexter), for example, remain scarce and with only a few examples reported to date.[17,32,35–36] In the case of Re(I), sensitisation has been predominantly studied for NIR emitting lanthanoids, with the rationale that the relatively red-shifted emission of tricarbonyl Re(I) diimine-type complexes makes them inefficient donors for visible emitters. In fact, the few examples of molecular systems containing both Re(I) and Eu(III) have been reported as having negligible sensitisation, if any at all, for Eu(III) luminescence.[37] The only example of Re(I)→Eu(III) ET was reported by Sørensen, Faulkner and co-workers;[38] however, the Re(I) donor is bound to separate pyridine ligands rather than a diimine system, causing a significant blue-shift of its ^{3}MLCT excited state to 420 nm, which lies well above the $^5D_1$ and $^5D_0$ excited states of Eu(III). While the ET was not quantified in their work, from the decrease in the excited state lifetime τ of the ^{3}MLCT in the absence or presence of Eu(III), its efficiency can be estimated to be around the 6-8% range.

We have previously reported the synthesis of a triangular assembly featuring three tricarbonyl Re(I) complexes bound to three (pyrid-2-yl)tetrazolato ligands.[39] The assembly displayed a relatively blue-shifted emission at 498 nm when compared to neutral tricarbonyl Re(I) diimine complexes. For this reason, we thought to investigate its ability to act as a sensitiser for both red-emitting Eu and NIR-emitting Yb. To endow the assembly with the capacity to bind Ln(III) ions, we constructed the triangular core using a previously reported ligand featuring a terpyridine functional group attached to the pyridine 4 position, 1*H*-(5-(2,2′:6′,2″-terpyridine)pyrid-2-yl)tetrazole,[40] Re_3L_3. A model structure obtained via density functional theory (DFT) for Re_3L_3 with the terpyridine units coordinated to Ln(III) nitrate complexes, $Re_3L_3Ln_3$, is shown in Figure 1 (where Ln = Lu). Extension of the ligand conjugation induces a red-shift of the ^{3}MLCT emission to 570 nm. Despite this red-shifted emission, this triangular assembly displays the first example of efficient sensitisation (90%) of Eu(III) luminescence, with a rate constant that is comparable to that observed for the sensitisation of NIR Yb(III) luminescence. Given this unprecedented result, we have endeavoured to elucidate the mechanism of sensitisation to identify structural features that would enable efficient ET between Re(I) and Eu(III). The investigation focused on comparing photophysical data at room temperature and 77 K.

Results and Discussion

The ligand LH, namely 4′-(5-(1*H*-tetrazol-5-yl)pyrid-5-yl)-2,2′:6′,2″-terpyridine, was prepared as previously reported.[40] The synthesis of the trinuclear Re_3L_3 complex was performed by reacting equimolar amounts of $Re(CO)_5Br$ and LH in the presence of an excess of triethylamine in toluene at reflux. The targeted Re_3L_3 could be isolated via flash chromatography in moderate yields (39%). The formation of Re_3L_3 was confirmed by its ^{1}H-NMR spectrum (Figure S1). Three diagnostic peaks appear as singlets at 9.57, 9.47 and 9.36 ppm in $CDCl_3$, associated with the three H6 atoms on the pyridine rings directly conjugated to the tetrazolate substituents. The presence of the three peaks suggests a *syn-syn-anti* arrangement of the pyridyltetrazolate moieties as shown in the model structure in Figure 1. This feature was also observed in the crystal structure of the previously reported triangular core without the pendant terpyridine (terpy) moieties.[39] The remaining signals in the 9.00–7.30 ppm region are largely superimposed and more difficult to resolve, but the overall spectrum integrates for a total of 39 H atoms, consistent with the proposed structure. The solid-state IR spectrum of Re_3L_3 displays intense CO stretching peaks at 2029 and 1901 cm^{-1}, as typical for Re centres bound to three CO ligands in a *facial* configuration, with quasi-degenerate out-of-phase *A*′ and *A*″ modes. The formation of Re_3L_3 was further confirmed by elemental analysis and HRMS in ESI+ mode. For the latter, the observed and calculated isotopic distribution for $[Re_3L_3H]^+$ and $[Re_3L_3H_2]^{2+}$ are in agreement (Figure S2).

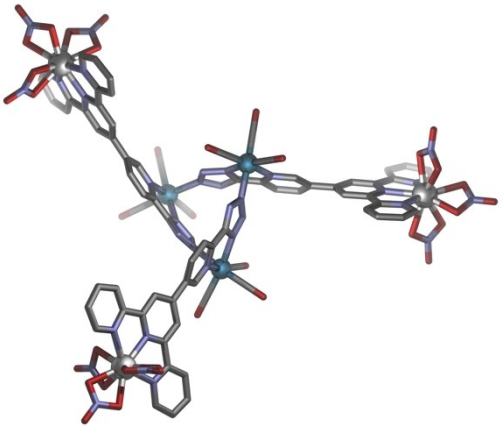

Figure 1. DFT model structure for $Re_3L_3Ln_3$ optimised using the function MPW1PW91 with mixed basis sets (D95 V/LANL2TZ(f)/Def2-QZVP). The structure was optimised using diamagnetic Lu(III) coordinated to the terpyridine moieties. Colour coding: silver spheres = Lu, teal spheres = Re, grey = C, blue = N, red = O; H atoms are omitted for clarity.

A summary of the photophysical properties for Re_3L_3 in the absence and presence of Ln(III) ions (Ln = Gd, Eu, Yb) is reported in Table 1. The UV-Vis spectrum of Re_3L_3 in diluted ($\approx 10^{-5}$ M) CH_2Cl_2 solution (Figures S3–S4) is comprised of intense bands at wavelengths shorter than 300 nm ($\varepsilon > 2x10^5$ $M^{-1}cm^{-1}$), mainly originating from intraligand (IL) $\pi\pi^*$ transitions. On the other hand, the shoulder above 300 nm is attributed to MLCT transitions, with partial admixture of ligand-to-ligand charge transfer (LLCT) character.[41] To confirm the assignment of the absorption bands, both static and time-dependent density functional theory (TDDFT) calculations were performed. The simulated absorption spectrum is shown in Figure S5, displaying features which match with the experimental spectrum (see

Table 1. Selected photophysical properties of Re_3L_3 and $Re_3L_3Ln_3$ (Ln = Gd, Eu, Yb) in CH_2Cl_2 solutions (*ca.* 10^{-5} M).

	abs. λ_{max} nm	^{3}MLCT λ_{em} nm	Ln λ_{em} nm	Φ	^{3}MLCT τ ns	k_{ET} 10^7 s^{-1}[a]	Φ_{ET}	Ln τ ms	^{3}MLCT τ (77 K) ms
Re_3L_3	280 325	520		0.059[a] 0.324[a,c]	524[d] 501.5[e] 2430[c,d]				
$Re_3L_3Gd_3$	293 330	570		0.050[a]	238[d] 221.6[e]				3.456
$Re_3L_3Eu_3$	293 330	570	527, 594, 618, 650, 686	0.30[a]	27[d] 22.0[e]	3.28[d] 4.09[e]	0.89[d] 0.90[e]	1.370[f]	0.080 (88%) 2.513 (12%)
$Re_3L_3Yb_3$	293 330	570	980	0.009[a] 0.013[b]	24[d] 21.2[e]	3.75[d] 4.27[e]	0.90[d] 0.90[e]	0.011[f]	0.854 (80%) 4.944 (20%)

[a] Visible photoluminescence quantum yield measured against an air-equilibrated aqueous solution of $[Ru(bpy)_3]Cl_2$ (Φ = 0.042).[42] [b] NIR photoluminescence quantum yield measured against an air-equilibrated toluene solution of $[Yb(phen)(tta)_3]$ (Φ = 0.016).[43] [c] Measured in degassed CH_2Cl_2 solution. [d] Measured by time-correlated single photon counting (TCSPC). [e] Measured by transient absorption (TA). [f] Measured by multichannel scaling (MCS).

Table S1 for a list of transitions and Figure S6 for orbital contours).

Upon excitation of the MLCT manifold at 375 nm, a CH_2Cl_2 solution containing Re_3L_3 displays blue-green emission. The emission spectrum (Figure 2, blue trace) comprises a featureless broad band with maximum at 520 nm, which is typical of radiative decay from excited states having charge transfer character. The excited state decay data in air-equilibrated solution, measured by time-correlated single photon counting (TCSPC), fit with a monoexponential function and an associated lifetime value of τ = 524 ns (Figure S7, blue trace). Re_3L_3 also displays relatively efficient emission, with a photoluminescence quantum yield Φ around 6%. The values of τ and Φ are both enhanced upon degassing, reaching 2430 ns and 32%, respectively. This enhancement supports the triplet spin multiplicity for the phosphorescent emitting state of Re_3L_3, which is therefore ascribed to a ^{3}MLCT.

The addition of excess $Gd(NO_3)_3(DMSO)_n$ to a CH_2Cl_2 solution containing Re_3L_3 produces a red-shift of the IL and MLCT bands

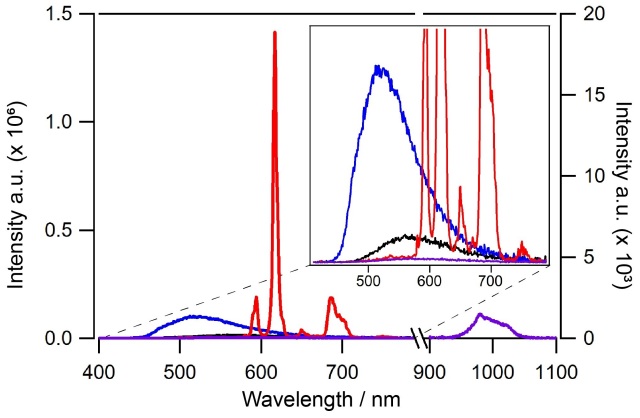

Figure 2. Emission spectra of Re_3L_3 (blue) and corresponding $Re_3L_3Ln_3$ complexes [Ln = Gd (black), Eu (red) and Yb (purple)] in CH_2Cl_2 solution. The NIR emission of $Re_3L_3Yb_3$ is arbitrarily normalised to the emission of Re_3L_3. All the solutions are excited 375 nm, corresponding to the ^{1}MLCT manifold.

in the absorption spectrum, suggesting coordination of Gd(III) ions to the terpy sites (Figure S3, red trace).[40] This assignment is again confirmed via TDDFT calculations (Figures S8–S9 and Table S2). Notably, the orbital contours of the LUMO + n (n = 0–2) extend now to include the π-conjugated system of the terpy moiety. Monitoring the change in absorbance while titrating $Gd(NO_3)_3(DMSO)_n$ into a Re_3L_3 solution (Figure S4) allows for the determination of the binding constants ($\log\beta_{11-13}$), which were *ca.* 7.0 ± 1.0, 12.5 ± 1.0 and 17.0 ± 1.0 for the first, second and third metals, respectively.[44] Lastly, the formation of the species $Re_3L_3Ln_3$ (Ln = Gd, Eu, Yb) is confirmed by HRMS in ESI + mode, again displaying consistent experimental and calculated patterns (Figures S10-S12).

The photophysical properties of $Re_3L_3Gd_3$ were initially studied to assess changes occurring upon coordination of Ln(III) ions to Re_3L_3 and in the absence of any sensitisation, since the lowest excited state $^6P_{7/2}$ of Gd(III) is too high in energy to act as an acceptor.[6] Excitation at 375 nm of a diluted CH_2Cl_2 solution containing $Re_3L_3Gd_3$ displays orange-red emission at room temperature, characterised by a featureless ^{3}MLCT band with a 50 nm red-shifted maximum at 570 nm (Figure 2). The red-shift is consistent with the trend in the absorption spectrum and is ascribed to stabilisation of the π* orbitals of the ligands upon coordination of the Gd(III) ions. Compared to Re_3L_3, the excited state decay lifetime τ reduces to 238 ns (Figure S7, red trace), with a photoluminescence quantum yield Φ determined around 5%. The observed changes upon coordination of the Gd(III) ions seem consistent with the energy gap law, whereby a red-shift in emission is accompanied by an enhancement of non-radiative decay pathways.[45] The ^{3}MLCT emission band of $Re_3L_3Gd_3$ was fit with a series of overlapping Gaussian functions, providing an estimated 0–0 transition energy of 19042 cm^{-1} (Figure S13).

The emission profile of an air-equilibrated CH_2Cl_2 solution containing $Re_3L_3Eu_3$, upon excitation at 375 nm, is shown in Figure 2 (red trace). The spectrum in the visible region is dominated by the typical line-like emission ascribed to radiative decay from the $^5D_0$ excited state to the corresponding ^7F_J states

(J = 0-4) of Eu(III). A characteristically weak peak at 527 nm is observed, which is attributed to emission from the $^5D_1$ excited state. Furthermore, the $^5D_0 \rightarrow {}^7F_0$ transition is barely visible, which provides further evidence of the highly symmetrical $Re_3L_3Eu_3$ species. The excited state decay lifetime τ, measured at 612 nm by multichannel scaling (MCS), fits monoexponentially with a value of 1.370 ms, which is typical for long-lived Eu(III) phosphorescence (Figure S14). A very weak broad band can be identified just above the baseline, which is consistent with residual emission from the ^{3}MLCT (Figure 2, red trace), and is similar to the emission band of $Re_3L_3Gd_3$. The calculated quantum yield for the Eu(III) emission is 30%. This value was obtained by subtracting the contribution of the residual ^{3}MLCT emission from the overall spectrum, which was obtained from the emission spectrum of $Re_3L_3Yb_3$ in the visible region (*vide infra*). Measurement of the excited state decay lifetime τ of the residual ^{3}MLCT emission at 570 nm (Figure S7) provides a value of 27 ns (TCSPC). Given the relatively weak intensity of the signal, the measurement was also confirmed using transient absorption (TA) (Figures S15-S17), which provided a consistent result of 22.0 ns. These values enable calculation of a sensitisation efficiency of 0.89 (TCSPC) or 0.90 (TA) and an ET rate constant k_{ET} of 3.28×10^7 s^{-1} (TCSPC) or 4.09×10^7 s^{-1} (TA).

Excitation at 375 nm of an air-equilibrated CH_2Cl_2 solution containing $Re_3L_3Yb_3$ reveals a very weak residual ^{3}MLCT band in the visible region and a band between 950 and 1050 nm in the NIR region, the latter being typical for the $^2F_{5/2} \rightarrow {}^2F_{7/2}$ transition of Yb(III) (Figure 2, purple line). A quantum yield $\Phi = 0.013$ was calculated for the NIR emission of Yb(III). The excited state decay of the Yb(III) emission was measured by MCS and monoexponential fitting with $\tau = 11$ μs (Figure S14). The maximum of the residual ^{3}MLCT emission is consistent with that of $Re_3L_3Gd_3$, with an excited state decay lifetime τ fit monoexponentially to a value of 24 ns, measured by TCSPC (Figure S7, green trace). A consistent value of 21.2 ns was obtained by TA (Figure S18). The ET rate constant k_{ET} was therefore determined to be 3.75×10^7 s^{-1} (TCSPC) or 4.27×10^7 s^{-1} (TA), and the sensitisation efficiency was calculated as 0.90 (both TCSPC and TA).

The collected photophysical data suggest that Re_3L_3 is an efficient sensitiser for Eu(III) and Yb(III) luminescence, both of which display a sensitisation efficiency of ≈90%. This conclusion is not completely unexpected for Yb(III), given the fact that the energy of the ^{3}MLCT excited state in $Re_3L_3Yb_3$ is well above the energy of the accepting $^2F_{5/2}$ excited state. Despite the large energy difference between the ^{3}MLCT and $^2F_{5/2}$ (10400 cm^{-1}) excited states ($\Delta E = 8628$ cm^{-1}), the observed efficient sensitisation is in line with previously reported complexes bearing Re(I) and Yb(III).[21–22,25,32,34–35] While there is virtually no spectral overlap between the emission of the Re_3L_3 donor and the absorption of the Yb(III) acceptor, the mechanism of Yb(III) sensitisation is usually postulated to proceed via an intermediate ligand-to-Yb charge transfer excited state[14,46] and/or phonon-assisted energy transfer.[47] However, such a high sensitisation efficiency from a ^{3}MLCT excited state of Re(I) to Eu(III) is unprecedented. The energy difference between the ^{3}MLCT and the $^5D_1$ (19028 cm^{-1}) or $^5D_0$ (17277 cm^{-1}) is relatively small, 14 cm^{-1} and 1765 cm^{-1}, respectively. We can postulate that energy is transferred from the ^{3}MLCT to $^5D_1$, according to ΔJ selection rules[14] and consistent with the fact that emission from the $^5D_1$ excited state is detected (Figure 2). Rapid $^5D_1 \rightarrow {}^5D_0$ internal conversion follows, but the occurrence of $^5D_0 \rightarrow {}^3$MLCT BET would be expected at room temperature given the low energy difference.[48] However, considering the long lifetime of the $^5D_0$ emission (1.370 ms), it must be concluded that BET is negligible in $Re_3L_3Eu_3$, if occurring at all. This conclusion is supported by the very low intensity of the residual ^{3}MLCT emission, similar to that observed for $Re_3L_3Yb_3$ where BET is not possible. The τ value is comparable to the previously reported excited state decay for the structurally similar complex LEu, 1.26 ms,[40] where energy transfer occurs directly from the ππ* excited state of the L ligand and no BET is detected on the basis of a complete absence of residual ligand-centred emission. In the LEu complex, sensitisation occurs with an efficiency of 48%, and the lack of BET is rationalised by the larger energy gap between the ligand ^{3}ππ* excited state, which mostly involves a terpy unit, and the $^5D_0$ excited state ($\Delta E = 4722$ cm^{-1}). Another notable observation in the present case is that the ET rate constants k_{ET} calculated for Eu(III) and Yb(III) are very similar, despite the fact that the mechanism of sensitisation are likely to be intrinsically different.[14]

To further investigate the energy transfer mechanism from the ^{3}MLCT to Eu(III) and Yb(III), the photophysical measurements were performed in a frozen matrix at 77 K. The emission spectrum of $Re_3L_3Eu_3$ (Figure S19) displays a more prominent and broad ^{3}MLCT band followed by the typical Eu(III) peaks. The excitation profiles monitored at 514 (^{3}MLCT) and 617 nm ($^5D_0 \rightarrow {}^7F_2$) confirm that Eu(III) sensitisation occurs via the ^{3}MLCT, as the shoulder between 360 and 450 nm is present in both spectra. The maximum of the ^{3}MLCT band appears blue-shifted when compared to the spectrum at room temperature. The increased energy of the ^{3}MLCT excited state is attributed to rigidochromism.[49] To determine the energy of the ^{3}MLCT 0–0 transition at 77 K, the emission band in the visible region of $Re_3L_3Yb_3$ was again fit with a series of overlapping Gaussian functions (Figure S20), providing a value of 21008 cm^{-1}. The excited state lifetime decays τ were recorded by TCSPC for the residual ^{3}MLCT emission of $Re_3L_3Gd_3$, $Re_3L_3Eu_3$ and $Re_3L_3Yb_3$ (Table 1 and Figure S21). In the case of Gd(III), a monoexponential decay was recorded with $\tau = 3.456$ ms. On the other hand, the values for Eu(III) and Yb(III) were both found to be biexponential with a dominant short component of 80 and 854 ns for Eu(III) and Yb(III), respectively. The minor longer-lived components were determined to be 2.513 and 4.944 ms, respectively. This longer-lived component is ascribed to ^{3}MLCT that is not quenched by sensitisation. From these data, the ET rate constant k_{ET} are calculated to be 1.22×10^7 and 8.82×10^5 s^{-1} for Eu(III) and Yb(III), respectively. Contrary to what is observed at RT, at 77 K the sensitisation of Yb(III) appears to be two order of magnitude slower than that of Eu(III).

By comparing the different photophysical data at RT and 77 K, the sensitisation mechanism of Eu(III) and Yb(III) at RT can be understood and modelled as two consecutive steps. Firstly, the ^{3}MLCT excited state transfers energy to the ^{3}ππ* excited

state of the terpy moiety. This is a thermally activated uphill ET ($\Delta E \approx +2958\ cm^{-1}$) and must be the rate-determining step of the sensitisation. The efficiency of this step might be facilitated by the fact that the orbital composition of the two excited states is similar (Figure S9). From the terpy $^3\pi\pi^*$ excited state, energy is rapidly transferred to Eu(III) or Yb(III), similarly to what was previously reported for the LEu and LYb complexes.[40] This two-step mechanism explains why the ET rate constant k_{ET} are very similar for Eu(III) and Yb(III) at RT. Direct energy transfer from the ^{3}MLCT to Eu(III) and Yb(III), if occurring at all, appears to be slower and outcompeted by ET between the ^{3}MLCT and the terpy $^3\pi\pi^*$ excited state. At 77 K, the ^{3}MLCT is raised in energy but still lies below the energy of the terpy $^3\pi\pi^*$ excited state ($\Delta E \approx +1000\ cm^{-1}$). Given the low temperature, ET between the ^{3}MLCT and the terpy $^3\pi\pi^*$ excited state is now excluded. Direct ET to Eu(III) and Yb(III) is the only viable pathway, which supports the two order of magnitude difference between the values of k_{ET}. The different mechanisms postulated at room temperature and 77 K are shown schematically in Figure 3 for $Re_3L_3Eu_3$.

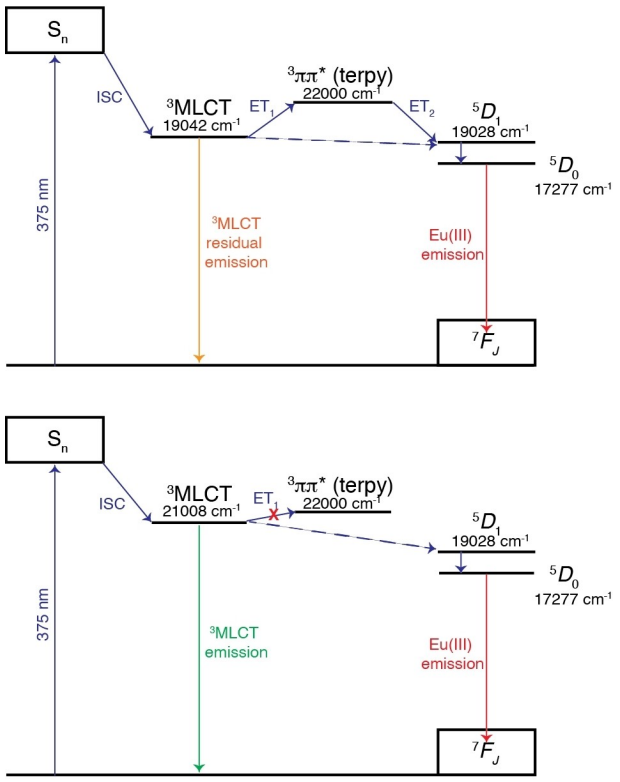

Figure 3. Schematised Jablonski diagram illustrating the different energy transfer mechanisms occurring at room temperature (top) and 77 K (bottom) for $Re_3L_3Eu_3$. ET_1 is the room temperature rate-determining energy transfer step from the ^{3}MLCT to the terpy $^3\pi\pi^*$ excited state, which is not occurring at 77 K.

Table 2. Energy transfer parameters for $Re_3L_3Eu_3$ at 77 K.

r Å	J_F cm^3M^{-1}	k_F s^{-1}]	J_D cm	H cm^{-1}
10.3	8.84×10^{-20}	1.58×10^{2}	5.14×10^{-3}	0.05

Modelling the direct ^{3}MLCT to Eu(III) energy transfer to both the Förster and Dexter mechanisms at 77 K was attempted, with calculated parameters provided in Table 2. To determine the overlap integrals, the ^{3}MLCT emission spectrum of $Re_3L_3Yb_3$ in the visible region and the absorption spectrum of a 0.1 M acetonitrile solution of $Eu(NO)_3(DMSO)_n$ were used. The Förster-based ET rate constant k_F was calculated by assuming a distance r between the donor and acceptor of 10.3 Å, taken as the distance between the two metal centres as determined from the DFT structure shown in Figure 1. The obtained data seem to rule out an energy transfer based on this mechanism, as the calculated rate constant is 3 orders of magnitude smaller than that determined experimentally. On the other hand, using the experimentally determined energy transfer rate constant and the overlap integral J_D, considering a Dexter mechanism, we find an electronic coupling H of 0.05 cm^{-1}. This value suggests the two metal centres are weakly coupled, with the presence of the fully conjugated ligand facilitating ET via a superexchange mechanism. These results are analogous to calculations performed by Ward and co-workers on Ru–Ln dyads (Ln = Nd, Er, Yb)[36] where the two metal centres were bridged by a p-conjugated ligand, suggesting that the direct ^{3}MLCT to Eu(III) energy transfer in $Re_3L_3Eu_3$ occurs via a ligand-assisted Dexter-type mechanism. The smaller k_{ET} for $Re_3L_3Yb_3$ is not surprising since ET in this complex cannot formally occur via Forster nor Dexter energy transfer, due to the lack of overlap between the emission of the donor and absorption of the acceptor. In this case, ET is ascribed to the previously mentioned charge transfer[14,46] and/or phonon-assisted mechanism.[47]

Conclusions

In this work, we have shown how the triangular assembly Re_3L_3 can be functionalised with terpy moieties to become an efficient antenna for the sensitisation of lanthanoid luminescence. The Re_3L_3 core has proven to be an efficient sensitiser for both Eu(III) and Yb(III) luminescence, and displaying the first example of efficient energy transfer (90%) between the Re(I)-centred ^{3}MLCT and Eu(III). Intriguingly, the rate constant for the sensitisation was found to be very similar for both Eu(III) and Yb(III). What seems to differentiate $Re_3L_3Ln_3$ from previously reported d-f assemblies is the two-step mechanism of sensitisation at room temperature, whose overall rate we believe is controlled by an initial uphill energy transfer between the ^{3}MLCT and the terpy $^3\pi\pi^*$ excited state. This step is then followed by rapid energy transfer to the corresponding Ln(III) excited state. This two step mechanism is supported by photophysical measurements at 77 K, where only direct sentisation from the ^{3}MLCT to Ln(III) is possible. In this case, sensititisation of Yb(III) is two orders of magnitude slower than that of Eu(III). Attempts to model the direct energy transfer at 77 K suggests that the sensitisation occurs via a superexchange ligand-mediated mechanism; although the limitation of this model in arbitrarily setting the distance between the donor and acceptor and the distance between the two metal centres should be considered. The unique $Re_3L_3Ln_3$ structure has

provided new insights into the sensitisation of lanthanoid luminescence from the charge transfer state of a coordination compound, and in particular provides a strategy to enable efficient Re(I) to Eu(III) energy transfer.

Supporting Information

The authors have cited additional references within the Supporting Information.[50–62]

Acknowledgements

The Australian Research Council is acknowledged for funding (DP240103097). The Pawsey Supercomputing Centre is acknowledged for the provision of computational resources. Open Access publishing facilitated by Curtin University, as part of the Wiley - Curtin University agreement via the Council of Australian University Librarians.

Conflict of Interests

The authors declare no conflict of interest.

Data Availability Statement

The data that support the findings of this study are available in the supplementary material of this article.

Keywords: europium · ytterbium · rhenium · luminescence · sensitisation

[1] S. V. Eliseeva, J.-C. G. Bünzli, *Chem. Soc. Rev.* **2010**, *39*, 189–227.
[2] J.-C. G. Bünzli, S. V. Eliseeva, *Chem. Sci.* **2013**, *4*, 1939–1949.
[3] D. Parker, J. D. Fradgley, K. L. Wong, *Chem. Soc. Rev.* **2021**, *50*, 8193–8213.
[4] G. Tessitore, G. A. Mandl, S. L. Maurizio, M. Kaur, J. A. Capobianco, *RSC Adv.* **2023**, *13*, 17787–17811.
[5] Y. Hasegawa, Y. Kitagawa, T. Nakanishi, *NPG Asia Mater.* **2018**, *10*, 52–70.
[6] J.-C. G. Bünzli, S. V. Eliseeva, *Basics of Lanthanide Photophysics, Vol. 7*, Springer, Berlin, **2010**.
[7] S. I. Weissman, *J. Chem. Phys.* **1942**, *10*, 214–217.
[8] A. K. R. Junker, L. R. Hill, A. L. Thompson, S. Faulkner, T. J. Sorensen, *Dalton Trans.* **2018**, *47*, 4794–4803.
[9] G. A. Hebbink, S. I. Klink, L. Grave, P. G. B. O. Alink, F. C. J. M. van Veggel, *ChemPhysChem* **2002**, *3*, 1014–1018.
[10] M. Latva, H. Takalo, V. M. Mukkala, C. Matachescu, J. C. RodriguezUbis, J. Kankare, *J. Lumin.* **1997**, *75*, 149–169.
[11] D. Xu, C. Liu, J. Yan, S. Yang, Y. Zhang, *J. Phys. Chem. C* **2015**, *119*, 6852–6860.
[12] A. N. Carneiro Neto, R. T. Moura, A. Shyichuk, V. Paterlini, F. Piccinelli, M. Bettinelli, O. L. Malta, *J. Phys. Chem. C* **2020**, *124*, 10105–10116.
[13] L. Abad Galan, A. N. Sobolev, B. W. Skelton, E. Zysman-Colman, M. I. Ogden, M. Massi, *Dalton Trans.* **2018**, *47*, 12345–12352.
[14] M. D. Ward, *Coord. Chem. Rev.* **2010**, *254*, 2634–2642.
[15] M. D. Ward, *Coord. Chem. Rev.* **2007**, *251*, 1663–1677.
[16] F. Ferraro, D. Paez-Hernandez, J. A. Murillo-Lopez, A. Munoz-Castro, R. Arratia-Perez, *J. Phys. Chem. A* **2013**, *117*, 7847–7854.
[17] S. Faulkner, L. S. Natrajan, W. S. Perry, D. Sykes, *Dalton Trans.* **2009**, 3890–3899.
[18] F. F. Chen, Z. Q. Chen, Z. Q. Bian, C. H. Huang, *Coord. Chem. Rev.* **2010**, *254*, 991–1010.
[19] M. Tropiano, C. J. Record, E. Morris, H. S. Rai, C. Allain, S. Faulkner, *Organometallics* **2012**, *31*, 5673–5676.
[20] M. R. Sambrook, D. Curiel, E. J. Hayes, P. D. Beer, S. J. A. Pope, S. Faulkner, *New J. Chem.* **2006**, *30*, 1133–1136.
[21] S. J. A. Pope, B. J. Coe, S. Faulkner, *Chem. Commun.* **2004**, 1550–1551.
[22] L. J. Charbonniere, S. Faulkner, C. Platas-Iglesias, M. Regueiro-Figueroa, A. Nonat, T. Rodriguez-Blas, A. de Blas, W. S. Perry, M. Tropiano, *Dalton Trans.* **2013**, *42*, 3667–3681.
[23] A. M. Nonat, S. J. Quinn, T. Gunnlaugsson, *Inorg. Chem.* **2009**, *48*, 4646–4648.
[24] T. Lazarides, N. M. Tart, D. Sykes, S. Faulkner, A. Barbieri, M. D. Ward, *Dalton Trans.* **2009**, 3971–3979.
[25] S. J. A. Pope, B. J. Coe, S. Faulkner, R. H. Laye, *Dalton Trans.* **2005**, 1482–1490.
[26] S. J. A. Pope, B. J. Coe, S. Faulkner, E. V. Bichenkova, X. Yu, K. T. Douglas, *J. Am. Chem. Soc.* **2004**, *126*, 9490–9491.
[27] N. M. Tart, D. Sykes, I. Sazanovich, I. S. Tidmarsh, M. D. Ward, *Photochem. Photobiol. Sci.* **2010**, *9*, 886–889.
[28] M. Mehlstäubl, G. S. Kottas, S. Colella, L. De Cola, *Dalton Trans.* **2008**, 2385–2388.
[29] A. Jana, B. J. Crowston, J. R. Shewring, L. K. McKenzie, H. E. Bryant, S. W. Botchway, A. D. Ward, A. J. Amoroso, E. Baggaley, M. D. Ward, *Inorg. Chem.* **2016**, *55*, 5623–5633.
[30] F. F. Chen, Z. Q. Bian, Z. W. Liu, D. B. Nie, Z. Q. Chen, C. H. Huang, *Inorg. Chem.* **2008**, *47*, 2507–2513.
[31] N. M. Ali, V. L. MacLeod, P. Jennison, I. V. Sazanovich, C. A. Hunter, J. A. Weinstein, M. D. Ward, *Dalton Trans.* **2012**, *41*, 2408–2419.
[32] N. M. Shavaleev, G. Accorsi, D. Virgili, Z. R. Bell, T. Lazarides, G. Calogero, N. Armaroli, M. D. Ward, *Inorg. Chem.* **2005**, *44*, 61–72.
[33] J. Ni, L. Y. Zhang, Z. N. Chen, *J. Organomet. Chem.* **2009**, *694*, 339–345.
[34] F. Kennedy, N. M. Shavaleev, T. Koullourou, Z. R. Bell, J. C. Jeffery, S. Faulkner, M. D. Ward, *Dalton Trans.* **2007**, 1492–1499.
[35] W. S. Perry, S. J. A. Pope, C. Allain, B. J. Coe, A. M. Kenwright, S. Faulkner, *Dalton Trans.* **2010**, *39*, 10974–10983.
[36] T. Lazarides, D. Sykes, S. Faulkner, A. Barbieri, M. D. Ward, *Chem. Eur. J.* **2008**, *14*, 9389–9399.
[37] M. Bortoluzzi, D. Battistel, G. Albertin, S. Daniele, F. Enrichi, R. Rumonato, *Chem. Pap.* **2016**, *70*, 43–52.
[38] L. R. Hill, O. A. Blackburn, M. W. Jones, M. Tropiano, T. J. Sørensen, S. Faulkner, *Dalton Trans.* **2013**, *42*, 16255–16258.
[39] P. J. Wright, S. Muzzioli, B. W. Skelton, P. Raiteri, J. Lee, G. Koutsantonis, D. S. Silvester, S. Stagni, M. Massi, *Dalton Trans.* **2013**, *42*, 8188–8191.
[40] P. J. Wright, J. L. Kolanowski, W. K. Filipek, Z. Lim, E. G. Moore, S. Stagni, E. J. New, M. Massi, *Eur. J. Inorg. Chem.* **2017**, 5260–5270.
[41] R. A. Kirgan, B. P. Sullivan, D. P. Rillema, *Top. Curr. Chem.* **2007**, *281*, 45–100.
[42] K. Suzuki, A. Kobayashi, S. Kaneko, K. Takehira, T. Yoshihara, H. Ishida, Y. Shiina, S. Oishic, S. Tobit, *Phys. Chem. Chem. Phys.* **2009**, *11*, 9850–9860.
[43] M. P. Tsvirko, *Opt. Spectrosc.* **2001**, *90*, 669–673.
[44] P. Gans, A. Sabatini, A. Vacca, *Ann. Chim.* **1999**, *89*, 45–49.
[45] Y. R. Poh, S. Pannir-Sivajothi, J. Yuen-Zhou, *J. Phys. Chem. C* **2023**, *127*, 5491–5501.
[46] W. D. Horrocks, J. P. Bolender, W. D. Smith, R. M. Supkowski, *J. Am. Chem. Soc.* **1997**, *119*, 5972–5973.
[47] E. Mathieu, S. R. Kiraev, D. Kovacs, J. A. L. Wells, M. Tomar, J. Andres, K. E. Borbas, *J. Am. Chem. Soc.* **2022**, *144*, 21056–21067.
[48] J. N. McPherson, L. Abad Galan, H. Iranmanesh, M. Massi, S. B. Colbran, *Dalton Trans.* **2019**, *48*, 9365–9375.
[49] C. O. Ng, S. C. Cheng, W. K. Chu, K. M. Tang, S. M. Yiu, C. C. Ko, *Inorg. Chem.* **2016**, *55*, 7969–7979.
[50] G. A. Crosby, J. N. Demas, *J. Phys. Chem.* **1971**, *75*, 991–1024.
[51] B. S. K. Chong, E. G. Moore, *Inorg. Chem.* **2018**, *57*, 14062–14072.
[52] G. W. T. M. J. Frisch, H. B. Schlegel, G. E. Scuseria, M. A. Robb, J. R. Cheeseman, G. Scalmani, V. Barone, G. A. Petersson, H. Nakatsuji, X. Li, M. Caricato, A. V. Marenich, J. Bloino, B. G. Janesko, R. Gomperts, B. Mennucci, H. P. Hratchian, J. V. Ortiz, A. F. Izmaylov, J. L. Sonnenberg, D. Williams-Young, F. Ding, F. Lipparini, F. Egidi, J. Goings, B. Peng, A. Petrone, T. Henderson, D. Ranasinghe, V. G. Zakrzewski, J. Gao, N. Rega, G. Zheng, W. Liang, M. Hada, M. Ehara, K. Toyota, R. Fukuda, J. Hasegawa, M. Ishida, T. Nakajima, Y. Honda, O. Kitao, H. Nakai, T. Vreven, K. Throssell, J. A. Montgomery, Jr., J. E. Peralta, F. Ogliaro, M. J. Bearpark, J. J. Heyd, E. N. Brothers, K. N. Kudin, V. N. Staroverov, T. A. Keith, R. Kobayashi, J. Normand, K. Raghavachari, A. P. Rendell, J. C. Burant, S. S.

Iyengar, J. Tomasi, M. Cossi, J. M. Millam, M. Klene, C. Adamo, R. Cammi, J. W. Ochterski, R. L. Martin, K. Morokuma, O. Farkas, J. B. Foresman, D. J. Fox, *Gaussian 16, Revision C.01* **2016**, Gaussian, Inc., Wallingford CT.
[53] R. Dennington, T. A. Keith, John M. Millam *GaussView, Version 6.1* **2016**, Semichem Inc. Shawnee Mission, KS.
[54] C. Adamo, V. Barone, *J. Chem. Phys.* **1998**, *108*, 664–675.
[55] T. H. Dunning Jr.; P. J. Hay, *Modern Theoretical Chemistry, Vol. 3*, Plenum, New York, **1977**.
[56] A. W. Ehlers, M. Böhme, S. Dapprich, A. Gobbi, A. Höllwarth, V. Jonas, K. F. Köhler, R. Stegmann, A. Veldkamp, G. Frenking, *Chem. Phys. Lett.* **1993**, *208*, 111–114.
[57] P. J. Hay, W. R. Wadt, *J. Chem. Phys.* **1985**, *82*, 299–310.
[58] L. E. Roy, P. J. Hay, R. L. Martin, *J. Chem. Theory Comput.* **2008**, *4*, 1029–1031.
[59] X. Cao, M. Dolg, *J. Chem. Phys.* **2001**, *115*, 7348.
[60] R. Gulde, P. Pollak, F. Weigend, *J. Chem. Theory Comput.* **2012**, *8*, 4062–4068.
[61] A. V. Marenich, C. J. Cramer, D. G. Truhlar, *J. Phys. Chem. B* **2009**, *113*, 6378–6396.
[62] N. M. O'Boyle, A. L. Tenderholt, K. M. Langner, *J. Comb. Chem.* **2008**, *29*, 839–845.

Manuscript received: March 27, 2024
Accepted manuscript online: June 2, 2024
Version of record online: August 12, 2024